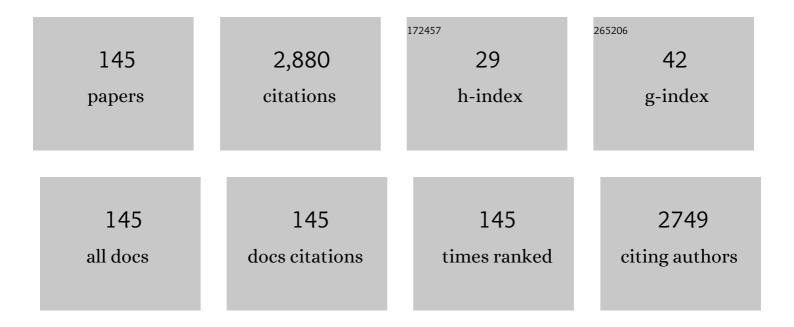
Jae-Suk Lee

List of Publications by Year in descending order

Source: https://exaly.com/author-pdf/5559509/publications.pdf Version: 2024-02-01



INE-SUR LEE

#	Article	IF	CITATIONS
1	Synthetic Control of Helical Polyisocyanates by Living Anionic Polymerization toward Peptide Mimicry. Macromolecules, 2022, 55, 1923-1945.	4.8	9
2	Influence of crosslinking in phosphoric acid-doped poly(phenylene oxide) membranes on their proton exchange membrane properties. Journal of Industrial and Engineering Chemistry, 2022, 107, 436-443.	5.8	13
3	Redox-active supercapacitor electrode from two-monomer-connected precursor (Pyrrole:) Tj ETQq1 1 0.784314 Electrochimica Acta, 2022, 415, 140243.	rgBT /Ove 5.2	erlock 10 Tf 50 27
4	Synthesis and photophysical properties of <i>N</i> -alkyl dithieno[3,2- <i>b</i> :2′,3′- <i>d</i>]pyrrole based donor/acceptor-Ï€-conjugated copolymers for solar-cell application. RSC Advances, 2022, 12, 17682-17688.	3.6	3
5	Hyperbranched Poly(Clycidol)â€Grafted Silica Nanoparticles for Enhancing Liâ€lon Conductivity of Poly(Ethylene Oxide). Macromolecular Materials and Engineering, 2021, 306, 2000572.	3.6	5
6	Antibacterial Polymeric Nanofibers from Zwitterionic Terpolymers by Electrospinning for Air Filtration. ACS Applied Nano Materials, 2021, 4, 2375-2385.	5.0	20
7	Impact of N-Substituent and p <i>K</i> _a of Azole Rings on Fuel Cell Performance and Phosphoric Acid Loss. ACS Applied Materials & Interfaces, 2021, 13, 531-540.	8.0	9
8	Preparation of a polymer nanocomposite <i>via</i> the polymerization of pyrrole : biphenyldisulfonic acid : pyrrole as a two-monomer-connected precursor on MoS ₂ for electrochemical energy storage. Nanoscale, 2021, 13, 5868-5874.	5.6	11
9	Clathrate Hydrate Inhibition by Polyisocyanate with Diethylammonium Group. Langmuir, 2021, 37, 4147-4153.	3.5	8
10	Folding of Sequence-Controlled Graft Copolymers to Subdomain-Defined Single-Chain Nanoparticles. Macromolecules, 2021, 54, 8829-8838.	4.8	10
11	Electrochemical properties of anthraquinone-containing polymer nanocomposite by nano-level molecular ordering. Polymer Chemistry, 2021, 12, 6154-6160.	3.9	7
12	Electrochemical properties of an activated carbon xerogel monolith from resorcinol–formaldehyde for supercapacitor electrode applications. RSC Advances, 2021, 11, 33192-33201.	3.6	11
13	Phosphoric acid doped triazole-containing cross-linked polymer electrolytes with enhanced stability for high-temperature proton exchange membrane fuel cells. Journal of Membrane Science, 2020, 595, 117508.	8.2	45
14	Effect of vinylphosphonic acid and polymer binders with phosphate groups on performance of high-temperature polymer electrolyte membrane fuel cell. Catalysis Today, 2020, 358, 333-337.	4.4	20
15	Coloration of colloidal polymer particles through selective extraction of Mie backscattering for cation-responsible colorimetric sensors. Journal of Colloid and Interface Science, 2020, 560, 894-901.	9.4	10
16	Crosslinked poly(allyl glycidyl ether) with pendant nitrile groups as solid polymer electrolytes for Li–S batteries. Electrochimica Acta, 2020, 362, 137141.	5.2	7
17	Decoupling Critical Parameters in Large-Range Crystallinity-Controlled Polypyrrole-Based High-Performance Organic Electrochemical Transistors. Chemistry of Materials, 2020, 32, 8606-8618.	6.7	26
18	Metal-free anionic polymerization of n-hexyl isocyanate catalyzed by phosphazene bases. Polymer Chemistry, 2020, 11, 6073-6080.	3.9	6

#	Article	IF	CITATIONS
19	Solution-State Long-Range Molecular Ordering in Poly(3-hexylthiophene). Langmuir, 2020, 36, 11028-11033.	3.5	0
20	Synthesis of bottlebrush block copolymers from bottlebrush polystyrene and bottlebrush random copolymer of I‰ â€endâ€norbornyl polymethacrylates and their selfâ€assembly. Journal of Polymer Science, 2020, 58, 2159-2167.	3.8	2
21	Nanocomposite Supercapacitor Electrode from Sulfonated Graphene Oxide and Poly(pyrrole-(biphenyldisulfonic acid)-pyrrole). ACS Applied Energy Materials, 2020, 3, 6743-6751.	5.1	32
22	Highly ordered supramolecular structure built from poly(4-(4-vinylphenylpyridine)) and 1,1′-ferrocenedicarboxylic acid via hydrogen bonding. Polymer Chemistry, 2020, 11, 2666-2673.	3.9	6
23	Facile Synthesis of Amphiphilic Bottlebrush Block Copolymers Bearing Pyridine Pendants via Click Reaction from Protected Alkyne Side Groups. Macromolecules, 2020, 53, 2209-2219.	4.8	11
24	Synthesis and characterization of ï€-bridged [A(DA`nD`)2] based small molecules with potential optoelectronic application. Synthetic Metals, 2020, 261, 116307.	3.9	3
25	Enhanced conductivity and stability of anion exchange membranes depending on chain lengths with crosslinking based on poly(phenylene oxide). Polymer, 2020, 192, 122331.	3.8	13
26	Dialkylthienosilole and N â€alkyldithienopyrroleâ€based copolymers: Synthesis, characterization, and photophysical study. Journal of Physical Organic Chemistry, 2020, 33, e4063.	1.9	6
27	Solid polymer electrolytes from double-comb Poly(methylhydrosiloxane) based on quaternary ammonium moiety-containing crosslinking system for Li/S battery. Journal of Power Sources, 2020, 450, 227690.	7.8	15
28	Azole structures influence fuel cell performance of phosphoric acid-doped poly(phenylene oxide) with azoles on side chains. Journal of Membrane Science, 2020, 605, 118096.	8.2	22
29	Enhancement of the Molecular Ordering via the Polymerization of 3,4â€Ethylenedioxythiopheneâ€Based Twoâ€Monomerâ€Connected Precursor with 4,4â€Biphenyldisulfonic Acid. Macromolecular Chemistry and Physics, 2020, 221, 2000019.	2.2	2
30	Fabrication of a composite anion exchange membrane with aligned ion channels for a high-performance non-aqueous vanadium redox flow battery. RSC Advances, 2020, 10, 5010-5025.	3.6	21
31	In Situ Incorporation of Hydrophobic Emissive Complexes in Monodisperse Copolymer Particles via Surfactant-free Emulsion Polymerization. Macromolecules, 2020, 53, 10097-10106.	4.8	1
32	Growth of close-packed crystalline polypyrrole on graphene oxide via in situ polymerization of two-monomer-connected precursors. Nanoscale, 2019, 11, 15641-15646.	5.6	14
33	Synthesis of ultrahigh molecular weight bottlebrush block copolymers of ω-end-norbornyl polystyrene and polymethacrylate macromonomers. Polymer, 2019, 177, 241-249.	3.8	17
34	Molecular-scale-ordered structures of isoindigo and bithiophene-based small molecules through hydrogen bonding. Synthetic Metals, 2019, 256, 116149.	3.9	3
35	Supramolecular Architecture of Molecular-Level-Ordered 1,1′-Ferrocenedicarboxylic Acid with Poly(4-vinylpyridine) for Bulk Magnetic Coupling. ACS Applied Polymer Materials, 2019, 1, 397-404.	4.4	3
36	End-Capping Reaction of Living Anionic Poly(benzyl methacrylate) with a Pentafluorophenyl Ester for a Norbornenyl-ω-End Macromonomer with a Long Flexible Spacer: Advantage in the Well-Controlled Synthesis of Ultrahigh-Molecular-Weight Bottlebrush Polymers. Macromolecules, 2019, 52, 4828-4838.	4.8	11

#	Article	IF	CITATIONS
37	Hydrogen Bonding-Mediated Phase Transition of Polystyrene and Polyhydroxystyrene Bottlebrush Block Copolymers with Polyethylene Glycol. Macromolecules, 2019, 52, 4349-4358.	4.8	19
38	Copolymer Particles with Incorporated Gold and Silver Nanoparticles to Absorb Shortâ€Wavelength Scattering in Fullâ€Color Photonic Glasses. Particle and Particle Systems Characterization, 2019, 36, 1900167.	2.3	6
39	Utilization of a Kinetic Principle of the Sequence-Controlled Anionic Copolymerization of Isocyanates toward Polyisocyanate Copolymers Encoded with Multiple Monomer Sequences. Macromolecules, 2019, 52, 3530-3542.	4.8	9
40	Selfâ€emulsion polymerization of amphiphilic monomers—a green route to synthesis of polymeric nanoscaffolds. Journal of Polymer Science Part A, 2019, 57, 1165-1172.	2.3	5
41	Synthesis of a Rod-rod Diblock Copolymer, Poly(3-hexylthiophene)-block-poly(furfuryl isocyanate), through the Anionic Polymerization with an Oxyanionic Macroinitiator. Chinese Journal of Polymer Science (English Edition), 2019, 37, 866-874.	3.8	1
42	Monolithic carbon xerogel with co-continuous hierarchical porosity <i>via</i> one-step, template- and catalyst-free hydrothermal reaction with resorcinol and formaldehyde. RSC Advances, 2019, 9, 9480-9485.	3.6	6
43	Preparation of polymer electrolyte membranes based on poly(phenylene oxide) with different side chain lengths of phosphonic acid. Journal of Polymer Science Part A, 2019, 57, 1180-1188.	2.3	17
44	Molecular Design of an Interfacially Active POSS-Bottlebrush Block Copolymer for the Fabrication of Three-Dimensional Porous Films with Unimodal Pore Size Distributions through the Breath-Figure Self-Assembly. Macromolecules, 2019, 52, 1912-1922.	4.8	13
45	Living Initiator-Transfer Anionic Polymerization of Isocyanates by Sodium Diphenylamide. Macromolecules, 2019, 52, 9354-9363.	4.8	3
46	ï‰-Norbornenyl Macromonomers: <i>In Situ</i> Synthesis by End-Capping of Living Anionic Polymers Using a Norbornenyl-Functionalized α-Phenyl Acrylate and Their Ring-Opening Metathesis Polymerization. Macromolecules, 2019, 52, 103-112.	4.8	23
47	Determination of complex dielectric function of CH ₃ NH ₃ PbBr ₃ perovskite cubic colloidal quantum dots by modified iterative matrix inversion method. Optics Express, 2019, 27, 20098.	3.4	4
48	Organic–inorganic hybrid perovskite quantum dots with high PLQY and enhanced carrier mobility through crystallinity control by solvent engineering and solid-state ligand exchange. Nanoscale, 2018, 10, 13356-13367.	5.6	71
49	Experimental Formulation of Photonic Crystal Properties for Hierarchically Self-Assembled POSS–Bottlebrush Block Copolymers. Macromolecules, 2018, 51, 3458-3466.	4.8	74
50	Synthesis of Amphiphilic Helix–Coil–Helix Poly(3-(glycerylthio)propyl) Tj ETQq0 0 0 rgBT /Overlock 10 Tf 50 Macromolecules, 2018, 51, 697-704.	227 Td (is 4.8	ocyanate)- <i>12</i>
51	Molecular ordering of A(D–A′–D) ₂ -based organic semiconductors through hydrogen bonding after simple cleavage of <i>tert</i> -butyloxycarbonyl protecting groups. New Journal of Chemistry, 2018, 42, 2557-2563.	2.8	14
52	Precise Synthesis of Bottlebrush Block Copolymers from ω-End-Norbornyl Polystyrene and Poly(4- <i>tert</i> -butoxystyrene) via Living Anionic Polymerization and Ring-Opening Metathesis Polymerization. Macromolecules, 2018, 51, 447-455.	4.8	50
50	Synthesis of Hard–Soft–Hard Triblock Copolymers, Poly(2-naphthyl glycidyl) Tj ETQq1 1 0.784314 rgBT /Ove		
53	ether]- <i>block</i> -poly(2-naphthyl glycidyl ether), for Solid Electrolytes. Macromolecules, 2018, 51, 2293-2301.	4.8	33
54	Enhancement of molecular-level ordering of isoindigo based organic materials through deprotecting of cleavable carbamate groups with long alkyl chains. Synthetic Metals, 2018, 246, 172-177.	3.9	9

#	Article	IF	CITATIONS
55	Propagation-Inspired Initiation of an Aliphatic Sodium Amidate for the Living Anionic Homo- and Copolymerization of Isocyanates: Access to the Multiblocky Sequence Distribution of Binary Comonomers. Macromolecules, 2018, 51, 10083-10094.	4.8	12
56	Molecular and kinetic design for the expanded control of molecular weights in the ring-opening metathesis polymerization of norbornene-substituted polyhedral oligomeric silsesquioxanes. Polymer Chemistry, 2018, 9, 5179-5189.	3.9	19
57	Facile preparation of blend proton exchange membranes with highly sulfonated poly(arylene ether) and poly(arylene ether sulfone) bearing dense triazoles. Journal of Membrane Science, 2018, 560, 58-66.	8.2	56
58	Preparation of perovskite-embedded monodisperse copolymer particles and their application for high purity down-conversion LEDs. Materials Horizons, 2018, 5, 1120-1129.	12.2	12
59	Fundamental Kinetics of Living Anionic Polymerization of Isocyanates Emerging by the Sodium Diphenylmethane-Mediated Initiation. Macromolecules, 2018, 51, 6771-6781.	4.8	9
60	Precise Synthesis of Functional Block Copolymers by Living Anionic Polymerization of Vinyl Monomers Bearing Nitrogen Atoms in the Side Chain. Macromolecular Chemistry and Physics, 2017, 218, 1600445.	2.2	5
61	In situ formation of molecular-scale ordered polyaniline films by zinc coordination. Nanoscale, 2017, 9, 6545-6550.	5.6	19
62	Enhancing the durability of filtration the ultrafine aerosol by electrospun polymer filter containing quaternary ammonium moiety. Polymer, 2017, 121, 211-216.	3.8	12
63	Modified hydrogels based on poly(2-hydroxyethyl methacrylate) (pHEMA) with higher surface wettability and mechanical properties. Macromolecular Research, 2017, 25, 704-711.	2.4	27
64	Synthesis and organic field effect transistor properties of isoindigo/DPP-based polymers containing a thermolabile group. RSC Advances, 2017, 7, 16302-16310.	3.6	27
65	Enhanced proton conductivity at low humidity of proton exchange membranes with triazole moieties in the side chains. Journal of Membrane Science, 2017, 523, 480-486.	8.2	43
66	Morphological Control over ZnO Nanostructures from Self-Emulsion Polymerization. Crystal Growth and Design, 2016, 16, 3905-3911.	3.0	12
67	Close-packed polymer crystals from two-monomer-connected precursors. Nature Communications, 2016, 7, 12803.	12.8	29
68	Anionic Polymerization of Reactive 3â€Chloropropyl Isocyanate. Macromolecular Symposia, 2015, 349, 85-93.	0.7	7
69	A facile method to synthesize [A′(D′AD) ₂]-based push–pull small molecules for organic photovoltaics. RSC Advances, 2015, 5, 66005-66012.	3.6	21
70	Direct C–H arylation synthesis of (DD′AD′DA′)-constituted alternating polymers with low bandgaps ar their photovoltaic performance. New Journal of Chemistry, 2015, 39, 4957-4964.	1d _{2.8}	15
71	Enhanced performance in isoindigo based organic small molecule field-effect transistors through solvent additives. Journal of Materials Chemistry C, 2015, 3, 5951-5957.	5.5	16

5

#	Article	IF	CITATIONS
73	Dual function of a living polymerization initiator through the formation of a chain-end-protecting cluster: density functional theory calculation. Physical Chemistry Chemical Physics, 2014, 16, 24929-24935.	2.8	12
74	Well-Defined Block Copolymers with Triphenylamine and Isocyanate Moieties Synthesized via Living Anionic Polymerization for Polymer-Based Resistive Memory Applications: Effect of Morphological Structures on Nonvolatile Memory Performances. Macromolecules, 2014, 47, 8625-8633.	4.8	11
75	CdS/C60 binary nanocomposite films prepared via phase transition of PS-b-P2VP block copolymer. Journal of Colloid and Interface Science, 2014, 417, 166-170.	9.4	4
76	A Model Chiral Graft Copolymer Demonstrates Evidence of the Transmission of Stereochemical Information from the Side Chain to the Main Chain on a Nanometer Scale. Macromolecules, 2014, 47, 2796-2802.	4.8	18
77	Synthesis of Novel Amphiphilic Polyisocyanate Block Copolymer with Hydroxyl Side Group. Macromolecules, 2014, 47, 1563-1569.	4.8	28
78	Synthesis and characterization of isoindigo-based polymers using CH-arylation polycondensation reactions for organic photovoltaics. Journal of Polymer Science Part A, 2014, 52, 2926-2933.	2.3	21
79	Effect of Biphenyl Spacers on the Anionic Polymerization of 2-(4′-Vinylbiphenyl-4-yl)pyridine. Macromolecules, 2014, 47, 6706-6714.	4.8	11
80	Enolate anionic initiator, sodium deoxybenzoin, for leading living natures by formation of aggregators at the growth chain ends. Journal of Polymer Science Part A, 2013, 51, 1742-1748.	2.3	13
81	Isoindigo-based small molecules for high-performance solution-processed organic photovoltaic devices: the electron donating effect of the donor group on photo-physical properties and device performance. Physical Chemistry Chemical Physics, 2013, 15, 15193.	2.8	41
82	Exploration of the Mechanism for Self-Emulsion Polymerization of Amphiphilic Vinylpyridine. Macromolecules, 2013, 46, 7166-7172.	4.8	16
83	Synthesis and characterization of low bandgap π-conjugated copolymers incorporating 4,7-bis(3,3′/4,4′-hexylthiophene-2-yl)benzo[c][2,1,3]thiadiazole units for photovoltaic application. Journal of Materials Chemistry A, 2013, 1, 10306.	10.3	36
84	End-group cross-linked large-size composite membranes via a lab-made continuous caster: enhanced oxidative stability and scale-up feasibility in a 50 cm2 single-cell and a 220 W class 5-cell PEFC stack. RSC Advances, 2013, 3, 24154.	3.6	3
85	Effect of substituted groups on the living anionic polymerization ofÂ2-vinylcarbazole derivatives. Polymer, 2013, 54, 5615-5625.	3.8	6
86	Novel amphiphilic homopolymers containing <i>meta-</i> and <i>para-</i> pyridine moieties with living characteristics and their self-assembly. Journal of Polymer Science Part A, 2013, 51, 3458-3469.	2.3	12
87	Corrections to "Demonstration of Addressable Organic Resistive Memory Utilizing a PC-Interface Memory Cell Tester―[Jan 13 51-53]. IEEE Electron Device Letters, 2013, 34, 468-468.	3.9	0
88	Thermally cross-linkable hole transporting polymer synthesized by living anionic polymerization for effective electron blocking and reduction of exciton quenching in multilayer polymer light emitting diodes. Polymer Chemistry, 2013, 4, 969-977.	3.9	33
89	Hollow flower micelles from a diblock copolymer. Nanoscale, 2013, 5, 11554.	5.6	7
90	Reversible conformation-driven order–order transition of peptide-mimic poly(n-alkyl isocyanate) in thin films via selective solvent-annealing. NPG Asia Materials, 2012, 4, e29-e29.	7.9	29

#	Article	IF	CITATIONS
91	"Governing initiation-supporting termination―in chiral poly(n-hexyl isocyanate). Chemical Communications, 2012, 48, 826-828.	4.1	17
92	Palladiumâ€Catalyzed Direct C–H Arylation of Thieno[3,4â€ <i>b</i>]pyrazines: Synthesis of Advanced Oligomeric and Polymeric Materials. European Journal of Organic Chemistry, 2012, 2012, 5540-5551.	2.4	51
93	Arrangement of C60 via the Selfâ€Assembly of Postâ€Functionalizable Polyisocyanate Block Copolymer. Macromolecular Rapid Communications, 2012, 33, 2029-2034.	3.9	12
94	Mechanistic Pathway for the Formation of Radial Polystyrenes Using Diacyl Chloride. Macromolecules, 2012, 45, 2675-2681.	4.8	4
95	"Helicity Inversionâ€+ Linkage Effects of Chiral Poly(<i>n</i> -hexyl isocyanate)s. Macromolecules, 2012, 45, 8961-8969.	4.8	20
96	Uniâ€molecular Hollow Micelles from Amphiphilic Homopolymer Poly(2â€(4â€vinylphenyl)pyridine). Small, 2012, 8, 1173-1179.	10.0	23
97	Molecular Level Ordering in Poly(2â€vinylpyridine). Advanced Materials, 2012, 24, 3253-3257.	21.0	30
98	Structural and Electrical Characterization of a Block Copolymerâ€Based Unipolar Nonvolatile Memory Device. Advanced Materials, 2012, 24, 385-390.	21.0	93
99	Surface-Grafted Rodlike Polymers: Adaptive Self-Assembled Monolayers and Rapid Photo-Patterning of Surfaces. Chemistry of Materials, 2011, 23, 3517-3524.	6.7	18
100	Chiroptical Properties of Graft Copolymers Containing Chiral Poly(<i>n</i> -hexyl isocyanate) as a Side Chain. Macromolecules, 2011, 44, 7917-7925.	4.8	22
101	Effects of Different Reactive Oxyanionic Initiators on the Anionic Polymerizaition ofn-Hexyl Isocyanate. Macromolecules, 2011, 44, 3211-3216.	4.8	24
102	Functionalization of amphiphilic coil-rod-coil triblock copolymer poly(2-vinylpyridine)-b-poly(n-hexyl) Tj ETQq0 0 C) rgBT /Ove	erlock 10 Tf :
103	Au/CdS Hybrid Nanoparticles in Block Copolymer Micellar Shells. Macromolecular Rapid Communications, 2010, 31, 1798-1804.	3.9	15
104	A selective and direct synthesis of 2-bromo-4-alkylthiophenes: Convenient and straightforward approaches for the synthesis of head-to-tail (HT) and tail-to-tail (TT) dihexyl-2,2â€2-bithiophenes. Tetrahedron Letters, 2010, 51, 4526-4529.	1.4	12
105	Facile oneâ€pot synthesis of linear and radial block copolymers of styrene and isoprene through a novel coupling agent by living anionic polymerization. Journal of Polymer Science Part A, 2010, 48, 2636-2641.	2.3	11
106	Desalination properties of a novel composite membrane prepared by electrospinning method. Desalination and Water Treatment, 2010, 15, 84-91.	1.0	4
107	Desalination properties of a novel composite membrane with a lamination method. Desalination and Water Treatment, 2010, 15, 190-197.	1.0	0

108 Effect of Solvent Composition on Transformation of Micelles to Vesicles of Rodâ[^]Coil Poly(n-hexyl) Tj ETQq0 0 0 rgBT/Overlock 10 Tf 50

#	Article	IF	CITATIONS
109	Synthesis and Characterization of Highly Fluorinated Cross-linked Aromatic Polyethers for Polymer Electrolytes. Chemistry of Materials, 2010, 22, 5500-5511.	6.7	45
110	Living Anionic Polymerization of Styrene Derivatives Containing Triphenylamine Moieties through Introduction of Protecting Group. Macromolecules, 2010, 43, 8400-8408.	4.8	29
111	The fabrication of nanopatterns with Au nanoparticles-embedded micelles via nanoimprint lithography. Nanotechnology, 2009, 20, 365301.	2.6	12
112	Wellâ€Organized CdS/C ₆₀ in Block Copolymer Micellar Cores. Macromolecular Rapid Communications, 2009, 30, 976-980.	3.9	17
113	Block copolymers containing pyridine moieties: Precise synthesis and applications. Reactive and Functional Polymers, 2009, 69, 470-479.	4.1	37
114	Living Anionic Polymerization of Isocyanate Containing a Reactive Carbamate Group. Macromolecules, 2009, 42, 3927-3932.	4.8	13
115	Au-Coated 3-D Nanoporous Titania Layer Prepared Using Polystyrene-b-poly(2-vinylpyridine) Block Copolymer Nanoparticles. Langmuir, 2009, 25, 3344-3348.	3.5	21
116	Formation of Intermicellar-Chained and Cylindrical Micellar Networks From an Amphiphilic Rodâ^'Coil Block Copolymer: Poly(<i>n</i> -hexyl isocyanate)- <i>block</i> -poly(2-vinylpyridine). Langmuir, 2009, 25, 7188-7192.	3.5	18
117	Reversibly interchangeable, chain-wrapped micelles and vesicles of an amphiphilic rod–coil block copolymer. Chemical Communications, 2009, , 4824.	4.1	18
118	Highly selective incorporation of SiO2 nanoparticles in PS-b-P2VP block copolymers by quaternization. Journal of Materials Chemistry, 2009, 19, 7322.	6.7	15
119	Self-Organization of an Amphiphilic Rodâ^'Coilâ^'Rod Block Copolymer into Liquid Crystalline, Substrate-Supported Monolayers and Bilayers. Macromolecules, 2008, 41, 3181-3189.	4.8	30
120	Synthesis of Amphiphilic Miktoarm Star Copolymers of Poly(n-hexyl isocyanate) and Poly(ethylene) Tj ETQq0 0 0	rgBT/Ove	erlock 10 Tf 50
121	Solvent-Induced Transition of Hollow Sphere to Giant-Tube from Amphiphilic Rod-Coil-Rod Triblock Copolymers of 2-Vinylpyridine and <i>n</i> -Hexyl Isocyanate. Journal of Nanoscience and Nanotechnology, 2007, 7, 3892-3895.	0.9	3
122	Quantitative in Situ Coupling of Living Diblock Copolymers for the Preparation of Amphiphilic Coilâ^'Rodâ^'Coil Triblock Copolymer Poly(2-vinylpyridine)-b-poly(n-hexyl) Tj ETQq0 0 0 rgBT /Overlock 10 Tf 50 2	2174Tøl (isc	ocy an ate)-b-po
123	Location Control of Au/CdS Nanoparticles in Block Copolymer Micelles. Langmuir, 2007, 23, 11425-11429.	3.5	40
124	Fabrication of an Open Au/Nanoporous Film by Water-in-Oil Emulsion-Induced Block Copolymer Micelles. Langmuir, 2007, 23, 12817-12820.	3.5	27
125	Liquid Crystalline Ordering in the Self-Assembled Monolayers of Tethered Rodlike Polymers. Journal of the American Chemical Society, 2007, 129, 7756-7757.	13.7	38
126	Living Anionic Polymerization of the Amphiphilic Monomer 2-(4-Vinylphenyl)pyridine. Macromolecules, 2007, 40, 8553-8559.	4.8	48

#	Article	IF	CITATIONS
127	Photoinduced behaviors of isocyanate-based azo molecular glass and polymer. Optical Materials, 2007, 29, 970-974.	3.6	9
128	The Effect of Alkyl Side Chain and Additives on the Anionic Polymerization of Isocyanates with Carbamate Group. Macromolecular Symposia, 2006, 240, 151-156.	0.7	6
129	Synthesis and Self-Assembly Studies of Amphiphilic Poly(n-hexyl) Tj ETQq1 1 0.784314 rgBT /Overlock 10 Tf 50 Copolymer. Macromolecules, 2006, 39, 5009-5014.	667 Td (ise 4.8	ocyanate)-bio 64
130	Induction of Helicity in Poly(n-hexyl isocyanate) with Terminal Chiral Residues. Macromolecules, 2006, 39, 5965-5966.	4.8	32
131	Synthesis of poly(2-vinyl pyridine)-b-poly(n-hexyl isocyanate) amphiphilic coil-rod block copolymer by anionic polymerization. Journal of Polymer Science Part A, 2005, 43, 607-615.	2.3	45
132	Unprecedented Control over Polymerization ofn-Hexyl Isocyanate using an Anionic Initiator Having Synchronized Function of Chain-End Protection. Journal of the American Chemical Society, 2005, 127, 4132-4133.	13.7	69
133	Generation of highly stable amidate anion in anionic polymerization of 3-(triethylsilyl)propyl isocyanate. Journal of Polymer Science Part A, 2004, 42, 933-940.	2.3	9
134	Synthesis of Well-Defined Rod-Coil-Rod Polyhexylisocyanate-block-polystyrene-block-polyhexylisocyanate via One-Pot Anionic Polymerization. Macromolecular Rapid Communications, 2003, 24, 571-575.	3.9	31
135	Synthesis of well-defined block copolymers of n-hexyl isocyanate with isoprene by living anionic polymerization. Polymer, 2003, 44, 3847-3854.	3.8	40
136	The Behavior of Surface Relief Grating Formation on Organic Glass Films Containing Azo Choromophores. Molecular Crystals and Liquid Crystals, 2001, 370, 143-146.	0.3	12
137	Synthesis of Poly(n-hexyl isocyanate) by Controlled Anionic Polymerization in the Presence of NaBPh4. Macromolecules, 2001, 34, 2408-2410.	4.8	80
138	Anionic polymerization of isocyanates with optical functionalities. Polymer, 2001, 42, 7979-7985.	3.8	29
139	Anionic Polymerization of Chiral Isocyanate and Influence of the Initiator on Changes in the Optical Activity. Macromolecular Rapid Communications, 2001, 22, 1041-1046.	3.9	26
140	Anionic Polymerization of Isocyanates with Optically Active Properties. Molecular Crystals and Liquid Crystals, 2001, 370, 189-192.	0.3	1
141	Anionic Living Polymerization of Monomers with Photo-Electronic Properties for Control of Polymeric Nano Architectures. Molecular Crystals and Liquid Crystals, 2000, 349, 9-14.	0.3	6
142	Ultra-Thin Zeolite Films Through Simple Self-Assembled Processes. Advanced Materials, 1999, 11, 497-499.	21.0	27
143	Anionic Living Polymerization of 3-(Triethoxysilyl)propyl Isocyanate. Macromolecules, 1999, 32, 2085-2087.	4.8	74
144	Ultra-Thin Zeolite Films Through Simple Self-Assembled Processes. Advanced Materials, 1999, 11, 497-499.	21.0	1

#	Article	IF	Citations
145	Improved NLO properties through a liquid crystal phase poling. AICHE Journal, 1997, 43, 2827-2831.	3.6	2